Journal of Natural Sciences Research
ISSN 2224-3186 (Paper) ISSN 2225-0921 (Online)
Vol.5, No.14, 2015
www.iiste.org

Attenuation Variability in Porous Media: Effects on Phase Delay and Quality Factor

James A. Adegoke[1], Emmanuel O. Joshua[1] & Olusegun O. Adewoyin* [2]
[1] Department of Physics, University of Ibadan, Ibadan, Nigeria.
[2] Department of Applied Geophysics, Covenant University, Ota, Nigeria
Correspondence: Olusegun O. Adewoyin, Department of Applied Geophysics, Covenant University, Ota, Nigeria.

Abstract
Electromagnetic methods of surveying involve the propagation of time varying low frequency electromagnetic fields in and over the earth. This gives rise to a secondary electromagnetic field and a resultant field which is picked up by suitable receiving coil. This research work modelled electromagnetic method of survey using a Cathode Ray Oscilloscope and a signal generator. This work was aimed at relating the effects of phase delay and the quality factor of a propagating signal to some properties of the homogeneous medium, like porosity (compaction), permeability and hydraulic conductivity. River bed sand was used as the sample, it was washed, oven dried, sieved into different grain sizes and the porosity was determined. Each sample was packed in a square box and connected to a signal generator and an oscilloscope. Two sinusoidal waves of the same frequency, but different amplitudes were sent from a signal generator and the measurement was taken at different frequencies. Graphs of frequency were drawn each against phase delay and Q – factor. Graphs of porosity were drawn each against phase delay and Q – factor. In conclusion, we observed that the porosity of a material increased with the decrease in the mixture of its grain size and signals were more attenuated at lower frequencies but as the frequency of the input signal was increased, the material became more permeable to the passage of the input signal.
Keywords: porosity, attenuation coefficient, phase delay, quality factor and electromagnetism

1. Introduction

Electromagnetic method of survey engages the induction principle to measure the electrical conductivity of the subsurface. The principle of operation of this method is as follows; a primary alternating electric current of known frequency and magnitude is passed through a transmitting coil creating a primary magnetic field in the region surrounding the coil. The eddy current generated in the subsurface in response to the primary current in turn, induces a secondary current in the subsurface conductor which results in an alternating secondary magnetic field that is picked by the receiving coil. The secondary field is distinguished from the primary field by a phase lag. The ratio of the magnitudes of the primary and secondary currents is proportional to the terrain conductivity. The depth of penetration is determined by the coil separation and orientation (Eze, 1996). Prominent among this method of survey is the Ground penetrating radar (GPR). This method uses a high frequency electromagnetic pulse transmitted from a radar antenna to probe the earth. The transmitted radar pulse reflected from various interfaces within the subsurface and this is in turn detected by the radar receiver. The need to eliminate possible interfering effects such as radio frequency transmitters, extensive metal structures by conducting laboratory test to confirm the presence of some natural resources, before a proper geophysical survey is conducted so as to prevent the waste of money, time and human resources is what necessitated this study. And also to use common laboratory equipment such as the cathode ray oscilloscope and signal generator to measure the changes in the responses of phase delay and quality factor of an output signal in relation to the passage of signals through a porous medium.

This research work modelled the principle of electromagnetic methods of survey in the laboratory, using the principles of Ground penetrating radar approach. In this work, the transmitter is the signal generator; the receiver is a cathode ray oscilloscope while the targets are sand of various grain sizes enclosed in an insulator square box. The varying dielectric properties of the sand will cause the transmitted signal to be reflected back to the oscilloscope. As a result, some parameters such as the relationships between attenuation and phase delay, attenuation and quality factor can be determined (Emmanuel, 2000). This is a function of the electrical properties of the materials in the square box and it will also affect the signal. Also, to determine the relationships between phase delay and frequency, Quality factor and frequency. In the work of Hsing–Ti et al.,(2012), they used the finite - difference time - domain method and turning bands to calculate the wave attenuation in sand and dust storms at the frequency of 10 – 100 GHz. The digitized models with a random process using the turning bands method are simulated for sand and dust particles. It was found that the particle size distribution function and equivalent particle radius are two major factors which would affect the wave attenuation in sand and dust storms.

2. Methodology

River bed sand was collected and used as the sample in this study. The sample was washed severally to get rid of any amount of clay and organic particles that may be present. It was sun-dried to remove water and moisture from it. It was then dried in an oven for 1 hour at a temperature of 150^0C.This was necessary to remove moisture and some micro organisms which cannot survive at a temperature that is this high (Adegoke, 2005). The sample was allowed to cool. It was separated to five grain sizes, using standard sieves of 300µm, 212µm, 150µm, 75µm and 63µm meshes. From these grain sizes, five others were obtained by mixing from the original five samples, pairs of samples in proportion of 20%:80%, 40%: 60%, 60%:40% and 80%: 20%. For example, mixture of 20% of sample with grain size of 300µm and 80% of sample with grain size of 212µm to obtain an entirely different sample composition. This was done for the remaining grain sizes. In all, we selected 10 samples which have distinct porosities.

The porosities of the samples labelled as; A, B, C, D, E, F, G, H, I, and J were determined according to standard procedure and were obtained as shown in Table 1.

A square box was designed with Turf-nor material (a very good insulator) which serves as the internal frame and Aluminium plates were used to cover the sides with inner dimension of $4cm\ x\ 4cm\ x\ 1cm$ .Each of the square box was filled with sand from each sample and sealed. One of the two leads from the signal generator was connected to one side of the aluminium plate on the square box and from the other (opposite) plate; a lead was connected to channel 1 of the oscilloscope. Also from the signal generator, a lead was connected directly to channel 2 of the oscilloscope. Hence two sinusoidal waves of the same frequency, but different amplitudes were sent from a signal generator, one goes directly to the detector, while the other signal was allowed to pass through the porous medium. Thus, creating an eddy current in the sample and the secondary signal is generated. The generated signal was attenuated. The two signals arriving at the detector are similar to two perpendicular signals of different amplitude and phase difference. These signals interact forming lissajous figures in which the shape and the number of loops depends on the phase angle and frequency ratio of the two signals. The arrangement is as shown in figure 1.

3. Theory

The minor axis, a, and the major axis, b were measured from the Lissajous figures on the oscilloscope. Phase angle was obtained from;

$$\theta = Sin^{-1}\left(\frac{a}{b}\right) \tag{1}$$

The anelastic damping of waves is described by a parameter called the quality factor, denoted by Q. The quality factor (Q) is defined as the fractional loss of energy per cycle i.e.(Lowrie, 1997)

$$\frac{2\pi}{Q} = -\frac{1}{E}\lambda\frac{dE}{dR} \tag{2}$$

Where dE is the energy lost in one cycle?
E is the total elastic energy stored in the wave,
λ is the wavelength of the wave and
R is the distance the wave travels (in this case, the thickness of the medium).

Equation (2) can be written as

$$\frac{dE}{E} = -\frac{2\pi dR}{Q\lambda} \tag{3}$$

It is conventional to measure damping by its effect on the amplitude of a signal, since the energy of a wave is proportional to the square of its amplitude, A.

i.e. $E \alpha A^2$ (4)

(Since: $\frac{dx}{x}$ = relative change in x, Dass et al.)

We can write equation (3) in differential form as

$$\frac{dE}{E} = \frac{2\,dA}{A} \tag{5}$$

On solving the differential equation, we get the damped amplitude of a wave at a distance R from its sources as

$$\frac{2\,dA}{A} = -\frac{2\pi dR}{Q\,\lambda} \tag{6}$$

Equation (6) reduces to

$$\frac{dA}{A} = -\frac{\pi\ dR}{Q\ \ \lambda} \tag{7}$$

Integrating both sides of the above equation

$$\int \frac{dA}{A} = -\int \frac{\pi dR}{Q\,\lambda} \tag{8}$$

Then, we have

$$\ln A = -\frac{\pi}{Q}\int \frac{dR}{\lambda} + c \tag{9}$$

$$= -\frac{\pi R}{Q\lambda} + c \tag{10}$$

Taking logarithm of the above equation gives

$$A = \exp\left(-\frac{\pi R}{Q\lambda} + c\right) \tag{11}$$

$$= \exp\left(-\frac{\pi R}{Q\lambda}\right).\exp c \tag{12}$$

But $\exp c = A_0$

Therefore, we have

$$A = A_0 \exp\left(-\frac{\pi R}{Q\lambda}\right) \tag{13}$$

$$\frac{A}{A_0} = \exp\left(-\frac{\pi R}{Q\lambda}\right) \tag{14}$$

$$\ln\left(\frac{A}{A_0}\right) = -\frac{\pi R}{Q\lambda} \tag{15}$$

Making Q, the subject from equation (15), we have

$$Q = -\frac{\pi R}{\ln\left(\frac{A}{A_0}\right)\lambda} \tag{16}$$

Where, A_o, is the amplitude of the wave at the source.

The displacement *x* as a function of time for a wave that is periodic is given by

$$x = A\cos(wt + \phi) \tag{17}$$

But $\theta = wt + \phi$ at $t = 0$, $\theta^0 = \phi$

Where ϕ = phase angle in radians

$$\phi(rad) = \frac{2\pi\theta^0}{360^0}$$

From equation (17), the velocity as a function of time for a periodic motion is given by

$$v = \frac{dx}{dt} = -wA\sin(wt + \phi) \tag{18}$$

From equation (18), at *t=0*,

$$v = -wA\sin\phi \tag{19}$$

The relationship between velocity and wavelength is given below;

$$v = f\lambda \tag{20}$$

Based on the above,

$$\lambda = -\frac{wA\sin\phi}{f} \tag{21}$$

$$= \frac{2\pi fA\sin\phi}{f}$$

$$\lambda = 2\pi A\sin\phi \tag{22}$$

Thus, the estimation of Quality factor, Q can be written as, (putting equation 22 into equation 16)

$$Q = -\frac{\pi R}{\ln\left(\frac{A}{A_0}\right)2\pi A\sin\phi} \tag{23}$$

Table 1:Table showing samples and their porosities.

Sample	A	B	C	D	E	F	G	H	I	J
Porosity, ϕ	0.26	0.28	0.29	0.32	0.34	0.36	0.39	0.41	0.42	0.43

Table 2: Table of attenuation, phase difference, phase delay and quality factor at porosity 0.26

Samples	Porosity	Freq(Hz)	Atten	ϕ (rad)	Phase Del	Q (10^{-3})
A	0.26	200	0.02	0.927	0.0738	8.03
		400	0.022	0.775	0.0308	8.58
		600	0.024	0.644	0.0171	9.28
		800	0.028	0.524	0.0104	9.99
		1000	0.03	0.412	0.6556	11.7
		2000	0.032	0.305	0.2427	14.7
		3000	0.033	0.201	0.1066	21.4
		4000	0.034	0.099	3.939	41.7

Table 3: Table of attenuation, phase difference, phase delay and quality factor at porosity 0.28

Samples	Porosity	Freq(MHz)	Atten	ϕ (rad)	Phase Del	Q (10^{-3})
B	0.28	200	0.022	0.775	0.0617	8.58
		400	0.034	0.775	0.0308	6.28
		600	0.044	0.644	0.0171	6.06
		800	0.056	0.524	0.0104	6.94
		1000	0.062	0.524	0.8339	6.42
		2000	0.071	0.412	0.3278	7.24
		3000	0.072	0.305	0.1618	9.48
		4000	0.073	0.201	7.996	13.9
		5000	0.073	0.099	3.151	40

Table 4: Table of attenuation, phase difference, phase delay and quality factor at porosity 0.29

Sample	Porosity	Freq(MHz)	Atten	ϕ (rad)	Phase Del	Q (10^{-3})
C	0.29	200	0.02	0.927	0.0738	8.03
		400	0.032	0.775	0.0308	6.52
		600	0.04	0.644	0.0171	6.46
		800	0.044	0.524	0.0104	7.29
		1000	0.053	0.524	0.8338	7.08
		2000	0.062	0.305	0.2427	10.4
		3000	0.067	0.201	0.1066	14.8
		4000	0.067	0.201	7.996	14.8
		5000	0.067	0.099	3.151	29.5

Table 5: Table of attenuation, phase difference, phase delay and quality factor at porosity 0.32

Sample	Porosity	Freq(MHz)	Atten	Φ (rad)	Phase Del	Q (10^{-3})
D	0.32	200	0.024	0.775	0.0617	8.02
		400	0.026	0.775	0.0308	7.62
		600	0.028	0.644	0.0171	8.29
		800	0.032	0.524	0.0104	9.04
		1000	0.036	0.412	0.6556	9.18
		2000	0.04	0.305	0.2427	12.6
		3000	0.042	0.201	0.1066	18
		4000	0.042	0.099	3.939	35.9
		5000	0.042	0.099	3.151	35.9

Table 6: Table of attenuation, phase difference, phase delay and quality factor at porosity 0.34

Sample	Porosity	Freq(MHz)	Atten	Φ (rad)	Phase Del	Q (10^{-3})
E	0.34	200	0.022	0.927	0.0738	7.48
		400	0.036	0.775	0.0308	6.02
		600	0.044	0.644	0.0171	6.06
		800	0.053	0.524	0.0104	7.08
		1000	0.06	0.412	0.6556	8.09
		2000	0.069	0.305	0.2427	9.79
		3000	0.069	0.201	0.1066	14.5
		4000	0.069	0.201	7.996	14.5
		5000	0.069	0.099	3.151	28.9

Table 7: Table of attenuation, phase difference, phase delay and quality factor at porosity 0.36

Sample	Porosity	Freq(MHz)	Atten	Φ (rad)	Phase Del	Q (10^{-3})
F	0.36	200	0.024	0.775	0.0617	8.02
		400	0.032	0.644	0.0256	7.54
		600	0.036	0.412	0.0109	10.3
		800	0.039	0.412	0.8195	9.71
		1000	0.044	0.305	0.4854	11.8
		2000	0.046	0.201	0.1599	17
		3000	0.048	0.099	5.251	32.8
		4000	0.046	0.099	3.939	33.8
		5000	0.044	0.099	3.151	34.8

Table 8: Table of attenuation, phase difference, phase delay and quality factor at porosity 0.39

Sample	Porosity	Freq(MHz)	Atten	Φ (rad)	Phase Del	Q (10^{-3})
G	0.39	200	0.026	0.927	0.0738	6.62
		400	0.036	0.775	0.0308	6.02
		600	0.046	0.644	0.0171	5.86
		800	0.058	0.644	0.0128	5.6
		1000	0.064	0.412	0.0656	7.72
		2000	0.071	0.305	0.2427	9.58
		3000	0.071	0.201	0.1066	14.2
		4000	0.073	0.201	7.996	13.9
		5000	0.073	0.099	3.151	27.7

Table 9: Table of attenuation, phase difference, phase delay and quality factor at porosity 0.41

Sample	Porosity	Freq(MHz)	Atten	Φ (rad)	Phase Del	Q (10^{-3})
H	0.41	200	0.024	0.927	0.0738	7.02
		400	0.026	0.644	0.0256	8.76
		600	0.03	0.412	0.0109	11.7
		800	0.032	0.305	0.6067	14.7
		1000	0.034	0.201	0.3199	20.9
		2000	0.034	0.099	7.877	41.7
		3000	0.032	0.099	5.251	43.5
		4000	0.032	0.099	3.939	43.5
		5000	0.032	0.099	3.151	43.5

Table 10: Table of attenuation, phase difference, phase delay and quality factor at porosity 0.42

Sample	Porosity	Freq(MHz)	Atten	Φ (rad)	Phase Del	Q (10^{-3})
I	0.42	200	0.047	0.895	0.0712	5.01
		400	0.048	0.735	0.0292	5.59
		600	0.051	0.595	0.0158	6.52
		800	0.058	0.456	0.9071	7.72
		1000	0.06	0.337	0.5363	10.2
		2000	0.068	0.222	0.1766	13.3
		3000	0.071	0.222	0.1178	13.1
		4000	0.071	0.11	4.376	28.3
		5000	0.068	0.11	3.501	28.7

Table 11: Table of attenuation, phase difference, phase delay and quality factor at porosity 0.43

Sample	Porosity	Freq(MHz)	Atten	ϕ (rad)	Phase Del	Q (10^{-3})
J	0.43	200	0.023	0.775	0.0617	8.33
		400	0.032	0.524	0.0209	9.04
		600	0.036	0.412	0.0109	10.3
		800	0.038	0.305	0.6067	13
		1000	0.039	0.201	0.3199	19
		2000	0.04	0.099	7.877	37.1
		3000	0.038	0.099	5.251	38.4
		4000	0.038	0.099	3.939	38.4
		5000	0.038	0.099	3.151	38.4

4. Results and Discussion

Figures 2 – 6, showed the graphs of phase delay versus frequency. The graphs revealed that the Phase delay increased with increase in frequency. The phase delay implies the time difference between the primary and the secondary signals getting to the receiver and this was responsible for the change in the orientation of the Lissajous figures with change in frequency. This implied that the medium in the square case attenuated the signal passing through it and the degree of the attenuation increased with increase in frequency. Generally, the graphs indicated a linear relationship between phase delay and Frequency.

Figures 7 – 11, showed the graphs of Quality factor versus frequency. The graphs showed that the Q – Factor increased with increase in frequency. Generally, these graphs exhibited a linear relationship between the Q – factor and the Frequency. This implied that the fractional loss in energy of the signal passing through the medium increased as the frequency increased. That is, the material medium resisted the passage of the signals through it. But, at some point, as the frequency increased, the energy loss in the signal began to reduce. This is because the material medium had become more permeable to the passing signal simply because of increase in porosity of the medium.

Figures 12 – 16 showed a linear relationship between attenuation and porosity. That is, at low frequencies, the material medium offered a proportional resistance to the passage of signal with increasing permeability. As the frequency increased further, increase in porosity brought about a decrease in attenuation. This implied that the permeability of the material medium to the flow of signal was enhanced at high frequency. This is as a result of the dielectric breakdown as explained earlier analogous to that experienced in a parallel plate capacitor.

The figures 17 - 21 on phase delay versus porosity showed that as the frequency increased, the time difference between the primary signal and the secondary signal increased before arriving at the receiver. This implied that the material medium did not allow the passage of signals at low frequencies but as the frequency increased it became more porous to the passage of signals.

The square case with aluminium plates on both sides is analogous to a parallel plate capacitor with a dielectric material, which in the case of the experiment is the sand sample. A dielectric is a non conducting material between the conducting plates of a capacitor. When any insulating material medium is subjected to a strong electric field, it experiences dielectric breakdown, a partial ionization that permits conduction through it. Dielectric breakdown occurs when the electric is so strong that electrons are ripped loose from their molecules and crash into other molecules, liberating more electrons. This is obvious in the experiment carried out; we saw that at low frequency, when the electric field was not strong enough to break an electron loose from its molecule, the material medium behaved as an insulator. But, when the frequency of the passing signal was increased; the electric field around the material medium became strong enough to break electrons from their molecules therefore, the material medium became conducting.

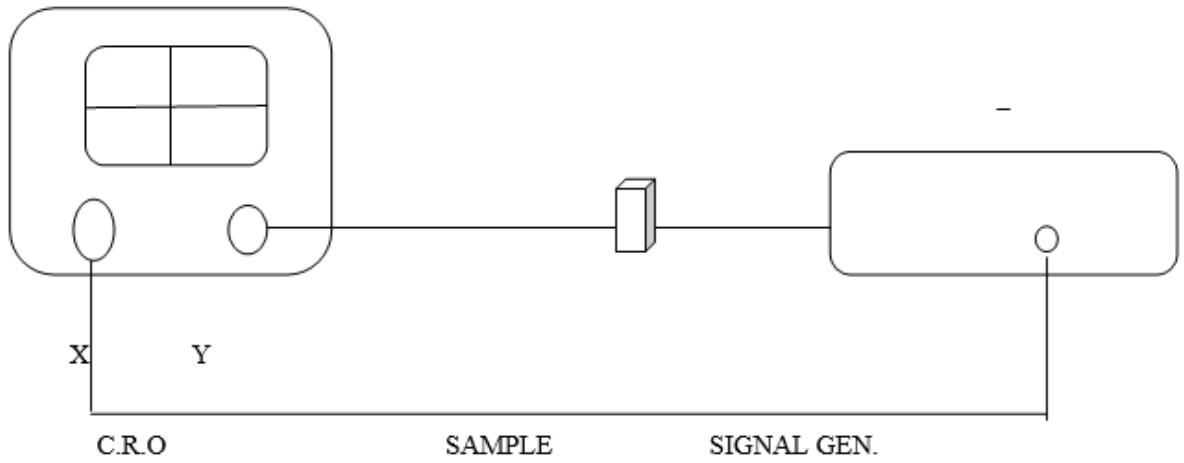

Figure 1: The block diagram of the experimental set up

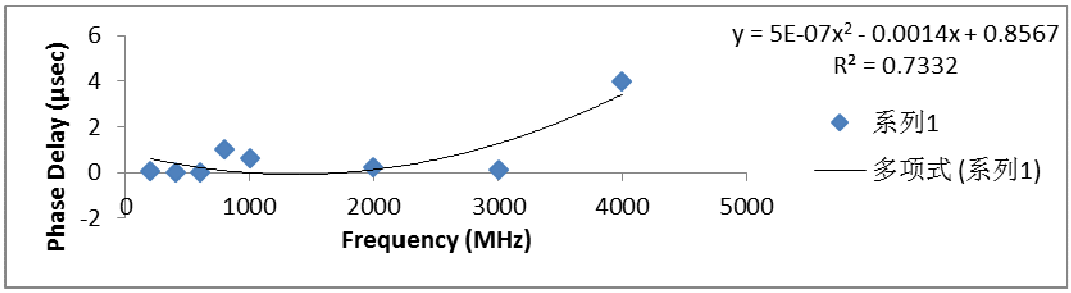

Figure 2: Graph of phase delay (µsec) versus frequency (MHz) at porosity 0.26

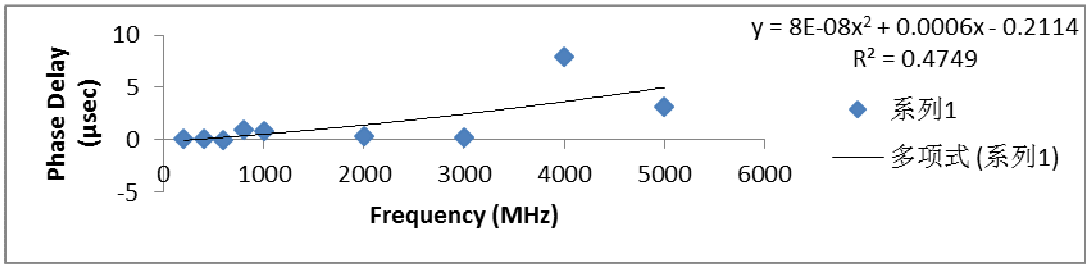

Figure 3: Graph of phase delay (µsec) versus frequency (MHz) at porosity 0.28

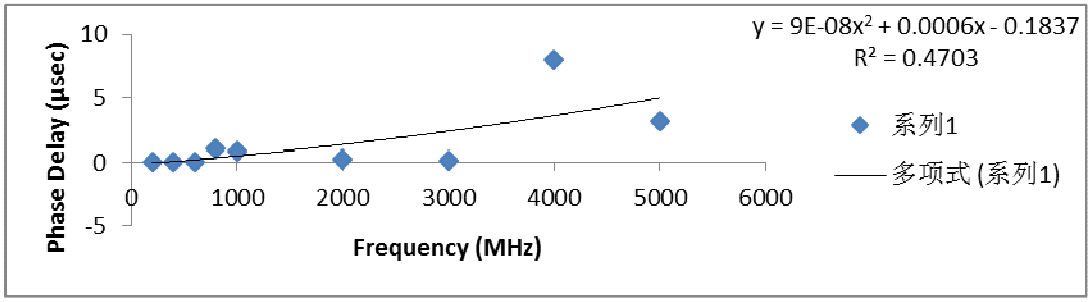

Figure 4: Graph of phase delay (µsec) versus frequency (MHz) at porosity 0.29

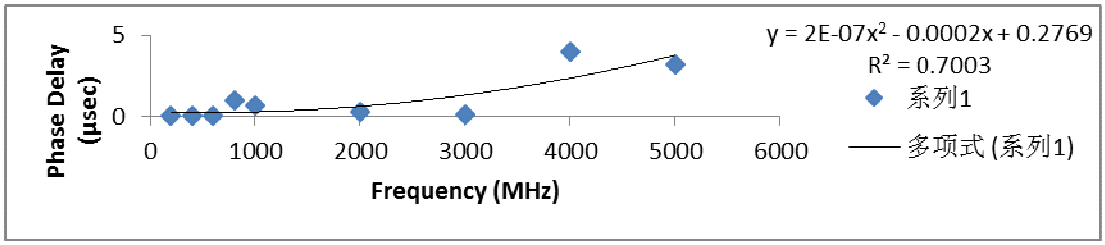

Figure 5: Graph of phase delay (µsec) versus frequency (MHz) at porosity 0.32

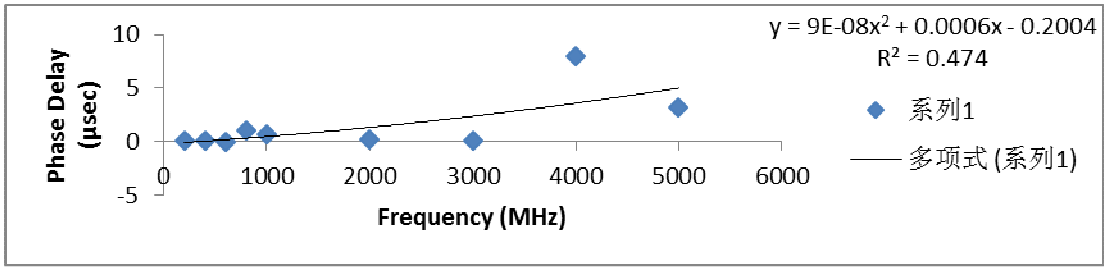

Figure 6: Graph of phase delay (µsec) versus frequency (MHz) at porosity 0.34

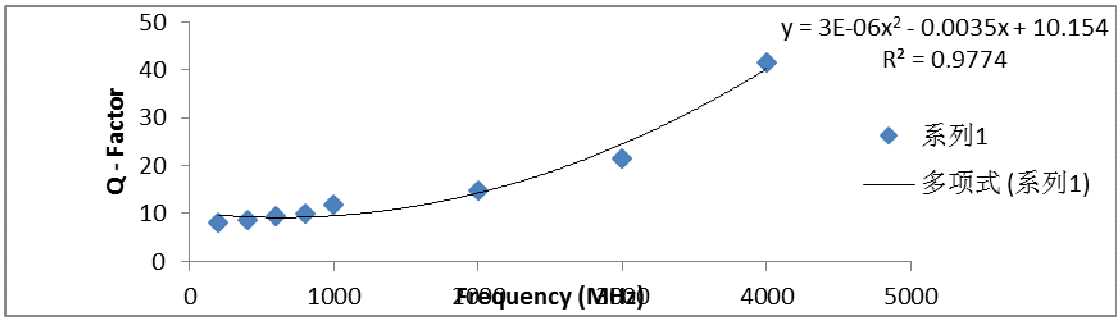

Figure 7: Graph Q – factor versus frequency (Hz) at porosity 0.26

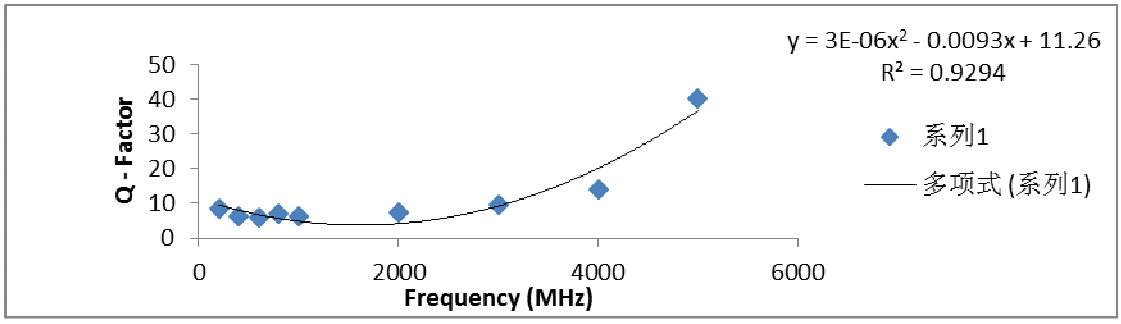

Figure 8: Graph Q – factor versus frequency (Hz) at porosity 0.28

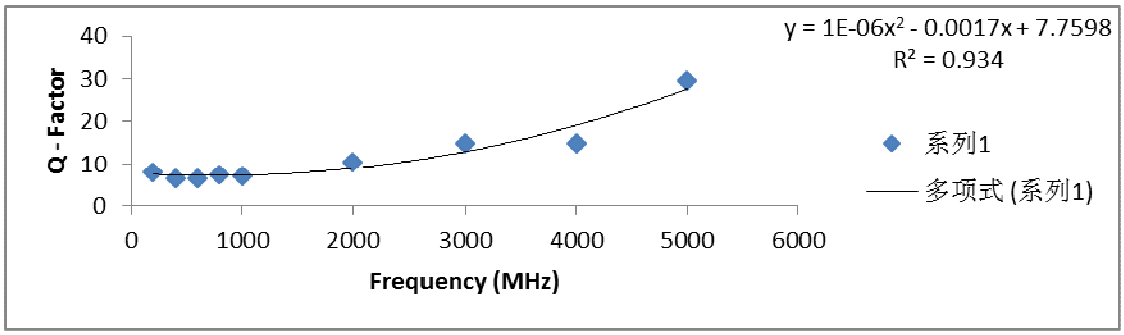

Figure 9: Graph Q – factor versus frequency (Hz) at porosity 0.29

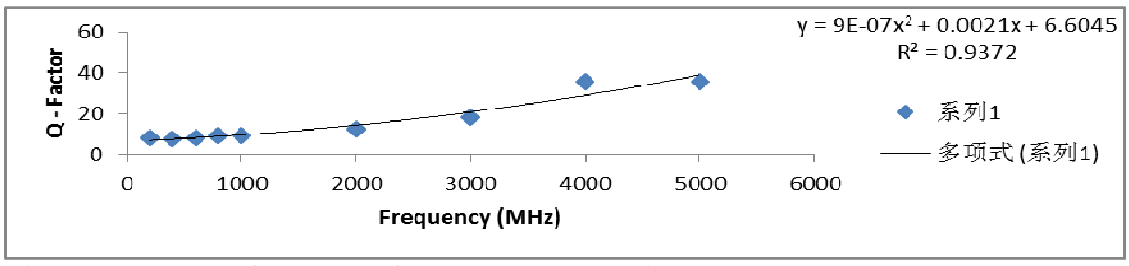

Figure 10: Graph Q – factor versus frequency (Hz) at porosity 0.32

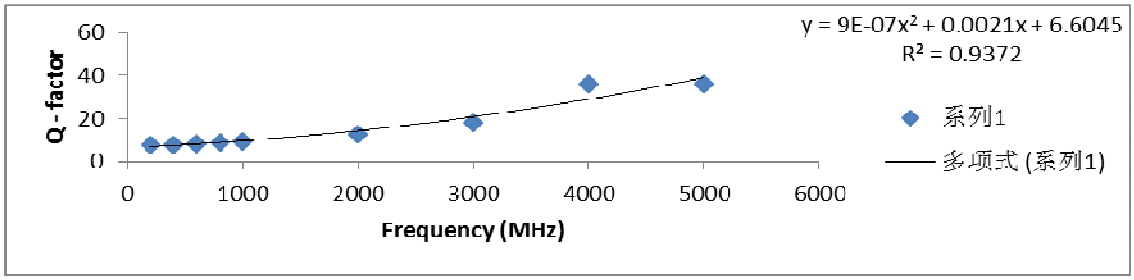

Figure 11: Graph Q – factor versus frequency (Hz) at porosity 0.34

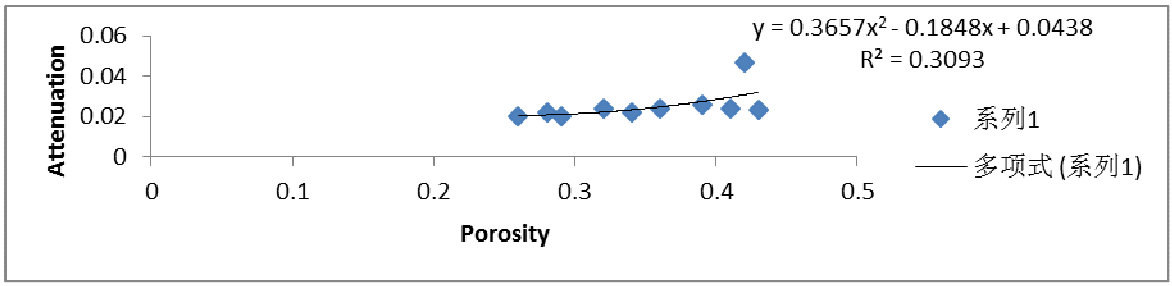

Figure 12: Graph of attenuation versus porosity at frequency 200MHz

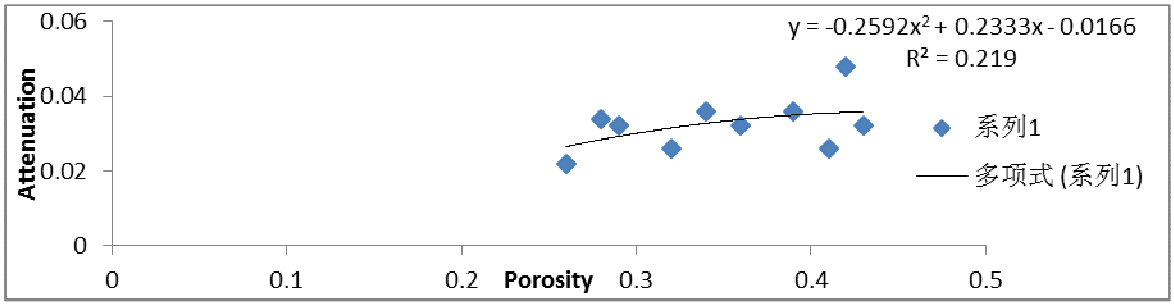

Figure 13: Graph of attenuation versus porosity at frequency 400MHz

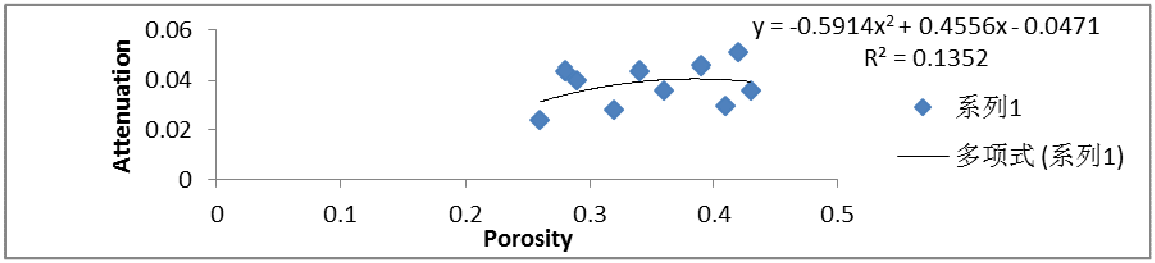

Figure 14: Graph of attenuation versus porosity at frequency 600MHz

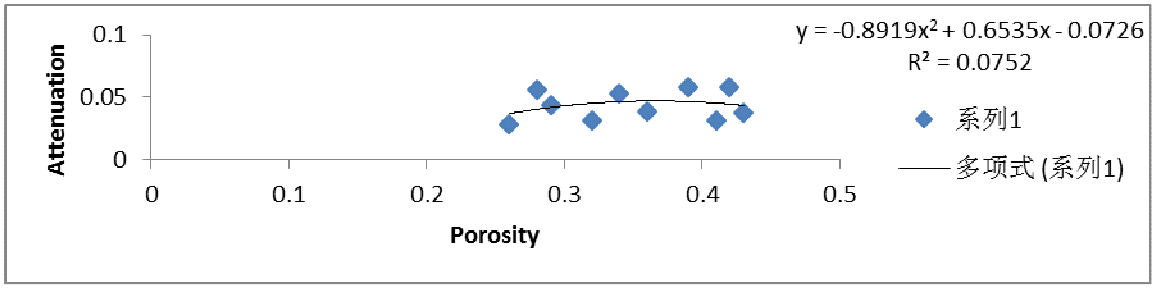

Figure 15: Graph of attenuation versus porosity at frequency 800MHz

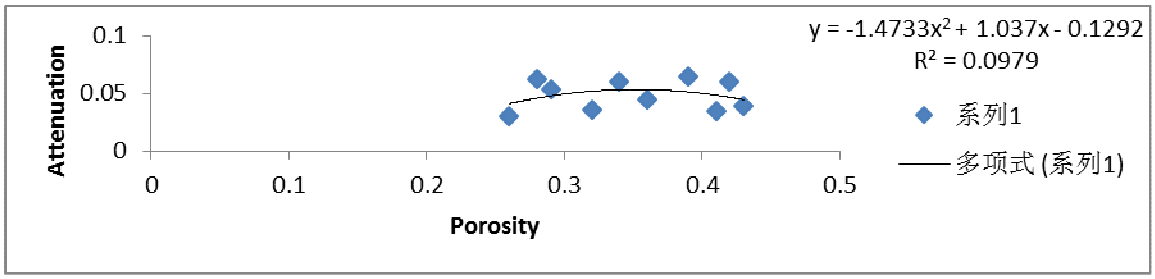

Figures 16: Graph of attenuation versus porosity at frequency 1000MHz.

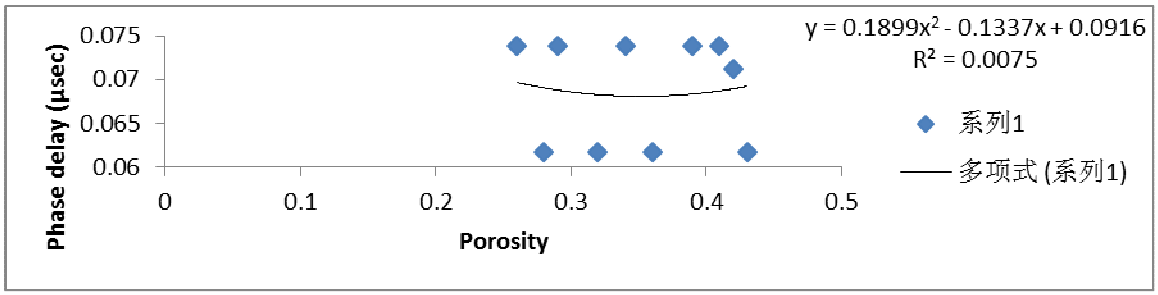

Figure 17: Graph of phase delay (µsec) versus porosity at frequency 200MHz

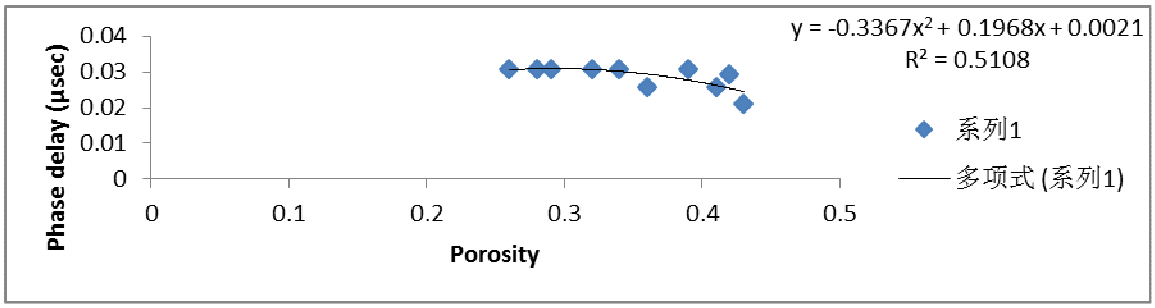

Figure 18: Graph of phase delay (µsec) versus porosity at 400MHz

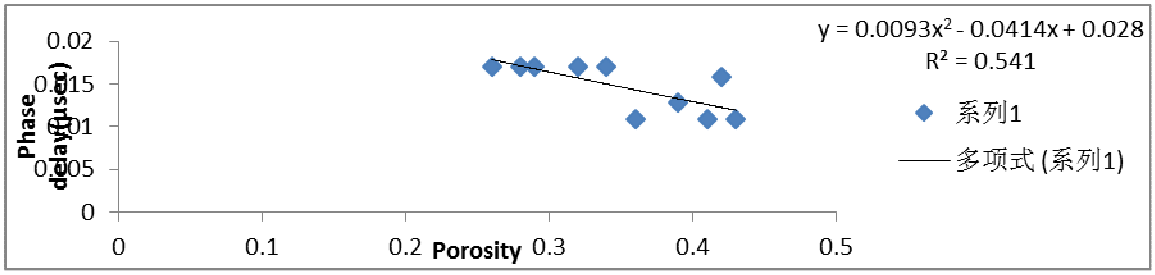

Figure 19: Graph of phase delay (µsec) versus porosity at 600MHz

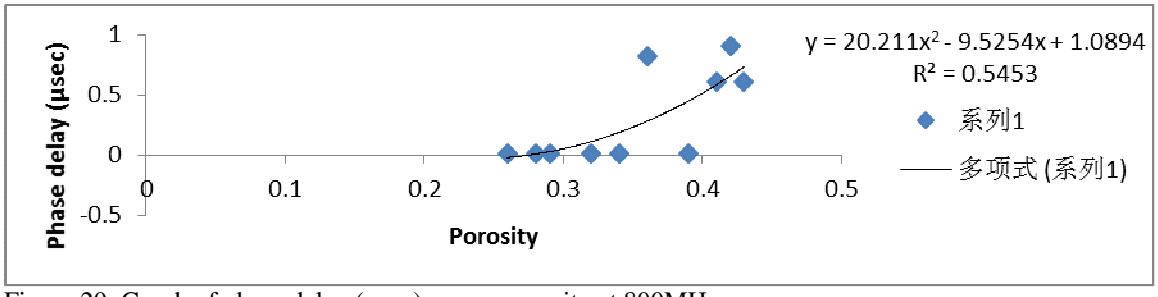

Figure 20: Graph of phase delay (µsec) versus porosity at 800MHz

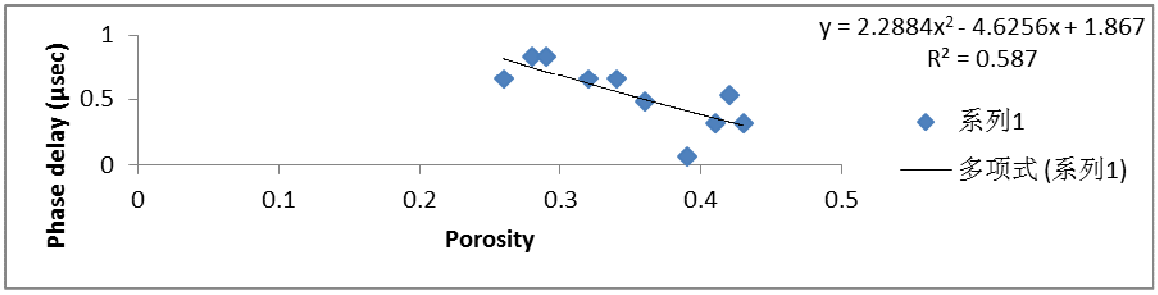

Figure 21: Graph of phase delay (µsec) versus porosity at 1000MHz

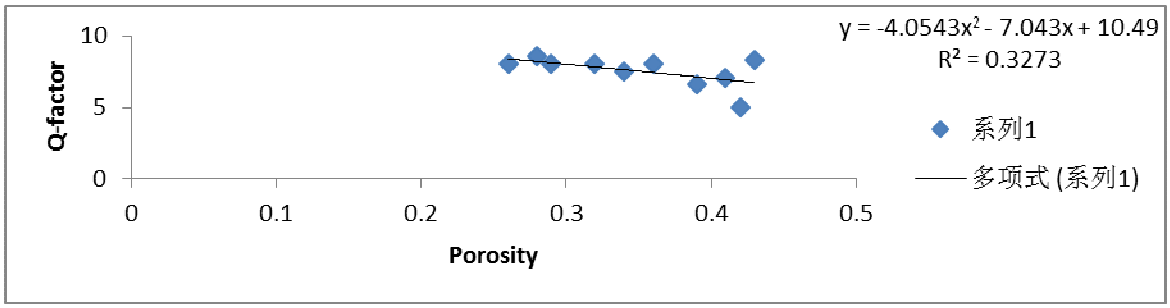

Figure 22: Graph of Q–factor versus porosity at frequency 200MHz

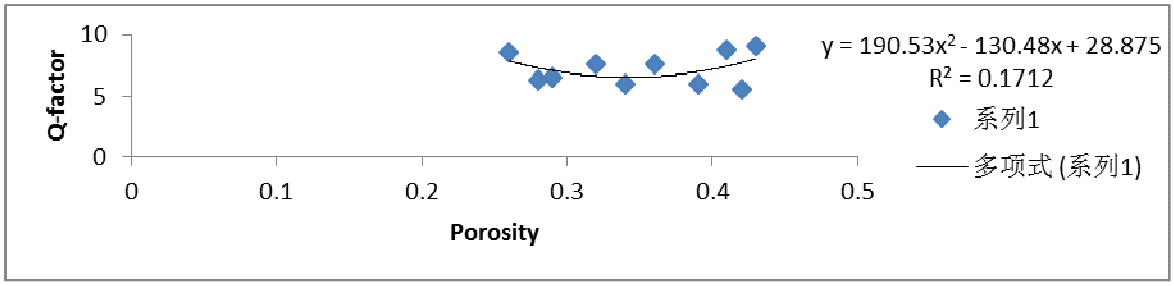

Figure 23: Graph of Q–factor versus porosity at frequency 400MHz

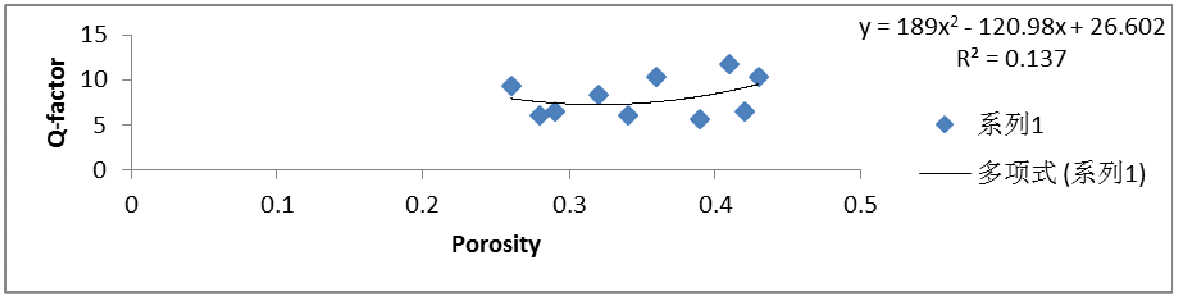

Figure 24: Graph of Q–factor versus porosity at frequency 600MHz

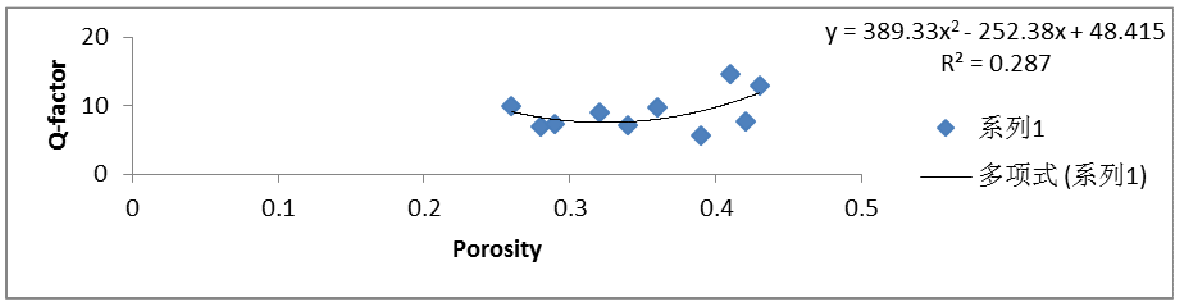

Figure 25: Graph of Q–factor versus porosity at frequency 800MHz

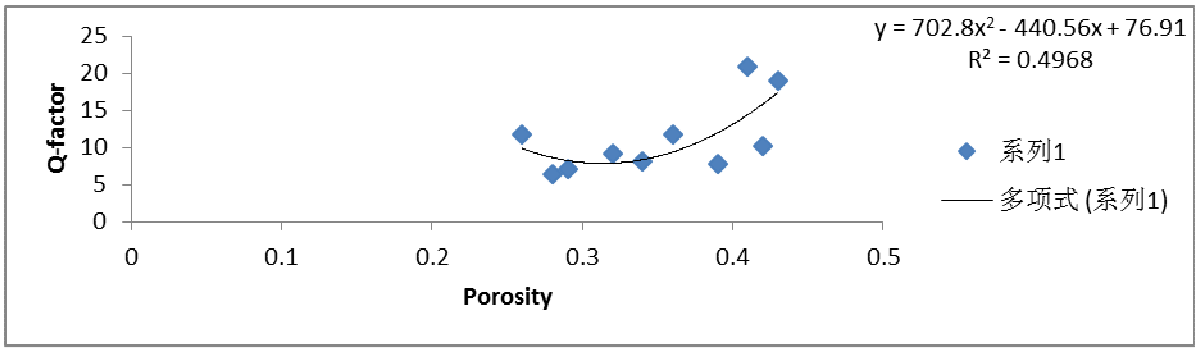

Figure 26: Graph of Q–factor versus porosity at frequency 1000

5. Conclusion

The principle of electromagnetic method of survey was modelled in the laboratory to examine the relationships between attenuation and porosity, phase delay and porosity, and also quality factor and porosity. Electromagnetic signals were more attenuated at lower frequencies but as the frequency of the input signal was increased, attenuation decreased. Attenuation increased with increase in porosity for input signal of frequency that is less than 0.7 MHz and also for operational frequency that is greater than 1.0MHz. Nevertheless, maximum attenuation (0.056-0.058) was experienced for input signal frequency in the range 0.8-1.0 MHz for materials of porosity 0.38. This may be related to the geometry/arrangement of the matrix of the medium at that porosity value among other factors.

References

Adegoke, J.A. (2005), "The effect of porosity, angle of hydrostatic equilibrium, volume flux and rate of groundwater flow through riverbed sand" Unpubl Ph. D thesis, Department of Physics, University of Ibadan

Emmanuel O.S. (2000), "Phase spectral analysis of broadband seismic waveforms propagated through three different rock samples" Unpubl. Ph.d Thesis, University of Ibadan.

Environmental geophysics (2011), "*Ground-penetrating radar*", [Online] November, 2011. Available from http:// www.epa.gov. [Accessed: 19th October, 2014]

Eze, J.O. (1996), "Electrical prospecting method for groundwater in crystalline basement areas of Nigeria" Unpubl. M.Sc. Thesis, University of Ibadan

Geophysical methods (2007), "*Electromagnetic surveys* [Online] 2007", Available from: http:// www.subsurfacesurvey.com. [Accessed: 19th October, 2014]

Hsing-Yi, C., & Chao-Cheng, K.. (2012), "Department of communication engineering, Yuan Ze Umo, Chingli, Taiwan".

Jackson, R. (2004), "Q-factor from wikipedia, the free encyclopedia. *Novel Sensors and Sensing"*.

Keary, P., Brooks, M., & Hill, I.(2002), "An introduction to geophysical exploration", Blackwell publishing.

Lowrie ,W. (1997), "Fundamentals of geophysics", Cambridge University Press.

Miller, C.D., Lial, M.L., & Schneider, D.I. (1990), "Ellipse, wikipedia, the free encyclopedia: fundamentals of college algebra", *Scott Foresman /Little* (3rd ed.) p. 381.

Milson, J. (2003), "Field Geophysics", 3rd ed.

Young, H.D., Freedam, R.A., & Sandin, T.R. (1998), "University Physics", *Addison-wesley*, (9th ed.).

The IISTE is a pioneer in the Open-Access hosting service and academic event management. The aim of the firm is Accelerating Global Knowledge Sharing.

More information about the firm can be found on the homepage:
http://www.iiste.org

CALL FOR JOURNAL PAPERS

There are more than 30 peer-reviewed academic journals hosted under the hosting platform.

Prospective authors of journals can find the submission instruction on the following page: http://www.iiste.org/journals/ All the journals articles are available online to the readers all over the world without financial, legal, or technical barriers other than those inseparable from gaining access to the internet itself. Paper version of the journals is also available upon request of readers and authors.

MORE RESOURCES

Book publication information: http://www.iiste.org/book/

Academic conference: http://www.iiste.org/conference/upcoming-conferences-call-for-paper/

IISTE Knowledge Sharing Partners

EBSCO, Index Copernicus, Ulrich's Periodicals Directory, JournalTOCS, PKP Open Archives Harvester, Bielefeld Academic Search Engine, Elektronische Zeitschriftenbibliothek EZB, Open J-Gate, OCLC WorldCat, Universe Digtial Library , NewJour, Google Scholar